

RESEARCH ARTICLE

View Article Online

View Journal | View Issue

Cite this: *Org. Chem. Front.*, 2024, **11**, 2468

Tetra-azobenzene extended calix[4]pyrroles: influence of photo-isomerization on chloride binding and its transport through liposomal membranes†‡

Pedro Ferreira, ^{a,b} Gemma Aragay ^{*a} and Pablo Ballester ^{*a,c}

In this work, we report the synthesis of three tetra-azobenzene extended calix[4]pyrroles and describe their photo-isomerization behavior in dichloromethane monitored by UV-Vis and NMR spectroscopies. We study and compare the binding properties of the receptors in their all-*trans* form and their corresponding photo-stationary state (PSS) *cis*-enriched mixtures with methyl trioctylammonium chloride (MTOA-Cl) in dichloromethane. Using ¹H NMR spectroscopy we probe that all the receptors form 1:1:1 ion-paired complexes with MTOA-Cl featuring a receptor separated geometry. Moreover, isothermal titration calorimetry (ITC) experiments enabled the accurate determination of the binding constants. Finally, we assess the chloride transport activity of the receptors by pre-inserting them in large unilamellar vesicles. We compare the results derived from the transport experiments with those of the binding studies in solution.

Received 1st March 2024,
Accepted 13th March 2024

DOI: 10.1039/d4qo00399c

rsc.li/frontiers-organic

Introduction

The dysregulation of ion transport across the cells' membrane can result in various medical conditions, including cystic fibrosis and renal diseases. The use of synthetic receptors that bind anions and facilitate their transport through liposomal membranes has been proposed as potential therapy for these diseases.^{1,2} There are numerous reported examples of synthetic receptors that can efficiently transport anions across the membranes of liposomes or cells.^{3,4} However, only a few examples are able to mimic the stimuli response behavior of proteins.^{5,6} This dynamic responsiveness would offer many advantages in the potential use of synthetic carriers operating autonomously in biological environments. Among the various external stimuli that can be applied for the modulation of the binding and transport properties of synthetic receptors, light is highly convenient due to its high spatial and temporal precision and lack of chemical waste generation.^{7,8}

We and others extensively studied calix[4]pyrroles (C[4]Ps) as privileged anion and ion-pair receptors in solution and more recently, used them as carriers of ions and small polar molecules across membranes.^{9–11} However, there are few reports on C[4]P scaffolds incorporating light-responsive units that cause significant changes in binding affinity upon switching.

In 2015, Cafeo *et al.* described the synthesis of a bis-calix[4]pyrrole receptor bearing an azobenzene unit as a linker.¹² They studied the photo-modulation of the binding affinity and selectivity of the receptor with a small series of dicarboxylate guests having a different number of methylene units between their two carboxylate ends. In DMSO solution, they observed a 100-fold difference in the binding constants for the succinate dianion between the *cis*- and *trans*-isomers of the receptor.

Recently, our group published several studies on derivatives of tetra-urea aryl-extended calix[4]pyrrole. These derivatives were equipped with four light- and pH-responsive units, such as azobenzene and spiropyran moieties. We aimed at regulating the uptake and release of molecular cargo from and on the surrounding solution by coupling the switching of the responsive units to the self-assembly of homo- and hetero-dimeric capsular aggregates.^{13–15}

We described in 2018 a tetra-azobenzene-extended calix[4]pyrrole receptor that is particularly relevant to this work.¹⁶ The thermal equilibration of the receptor in the dark provided the all-*trans* isomer featuring its four azobenzene units in *trans*-conformation (*tttt*-isomer). Irradiating the *tttt*-isomer with

^aInstitute of Chemical Research of Catalonia (ICIQ-CERCA), The Barcelona Institute of Sciences and Technology (BIST), Av. Països Catalans 16, 43007 Tarragona, Spain. E-mail: pballester@iciq.es, garagay@iciq.es

^bUniversitat Rovira i Virgili (URV), Departament de Química Analítica i Química Orgànica, c/Marcel·lí Domingo 1, 43007 Tarragona, Spain

^cICREA, Passeig Lluís Companys, 23, 08010 Barcelona, Spain

†Dedicated to Prof. Frank Würthner on the occasion of his 60th birthday.

‡Electronic supplementary information (ESI) available: General information and instruments, synthesis and characterization data, light irradiation studies, binding studies, calculations and anion transport studies. See DOI: <https://doi.org/10.1039/d4qo00399c>



365 nm light resulted in up to 85% partial isomerization of their azobenzene units, leading to a mixture of *cis*-enriched isomers (*cccc*-, *ccct*-, *ctct*-, *cctt*-, and *tttc*-) in the photo-stationary state (PSS). We investigated the binding properties of this receptor towards 4-phenyl pyridine *N*-oxide and tetramethylammonium 1,1'-biphenyl 4-carboxylate guests in dichloromethane and acetonitrile solution, respectively. We described that the binding affinity of the *cis*-enriched mixture of isomers decreased by one order of magnitude compared to the *all-trans*-counterpart for both guests and in the two solvents. We attributed this difference to additional CH- π and π - π interactions occurring between the 4-phenyl substituents of the included guests and the upper aromatic panels of the receptor azo-units in *trans*-conformation. Other tetra-azobenzene extended C[4]P have been previously reported, but their photo-isomerization behaviors and binding properties were not described.^{17,18}

Very recently, Wezenberg and co-workers reported the synthesis of a strapped calix[4]pyrrole receptor with a stiff-stilbene unit incorporated in the strap.¹⁹ The switching of the stilbene unit between its *Z* and *E* forms significantly reduced the size of the macrocyclic anion binding pocket delimited by the strap. This structural change translated into a large difference in binding constants of the two isomeric macrocycles for chloride in acetonitrile solution. The binding of the *E* isomer for chloride was almost 4 orders of magnitude larger than that of the *Z* counterpart. The reported difference in binding affinity is the largest known for a photo-switchable synthetic receptor for chloride. More recently, the same group reported an analogous receptor featuring a dithienylethene (DTE) unit in the strap.²⁰ The chloride binding constant was minimally affected by the photo-isomerization of the DTE unit between its ring-open and closed forms.

To the best of our knowledge, the properties of photo-responsive C[4]P receptors were not evaluated using photo-controlled anion transport experiments. Successful examples of photo-controlled anion transport experiments have been reported using tweezer-type receptors incorporating stiff-stilbene and azobenzene spacers. The anion binding sites of these receptors were mostly based on amides and (thio)ureas functions.^{21–23} In general, differences in binding constants of the two photo-isomers with chloride are thought to result in different transport activity.²⁴ However, in most cases, the difference in transport activity cannot be exclusively attributed to the different binding properties of the isomeric receptors. Several other factors like carrier deliverability and mobility within the membrane also play a crucial role in transmembrane transport studies. Therefore, more work needs to be done to gain a better understanding of the relationship between binding affinity and transport activity of photo-isomerizable receptors.

Herein, we report the synthesis and structural characterization of three “four-wall” *meso*-tetra-azobenzene-extended tetra-methyl calix[4]pyrrole receptors 1–3 featuring different substituents at their upper rims (Fig. 1). We used UV-Vis and NMR spectroscopy to monitor the photo-isomerization behav-

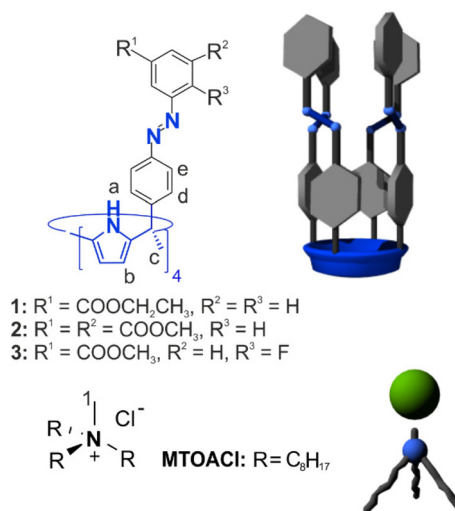


Fig. 1 Molecular structures and cartoon representations of the light responsive C[4]P 1–3 and MTOA-Cl ion-pair used in this work. Selected assignments of hydrogen atoms of the receptors and the MTOA-Cl guest are indicated.

ior of the *all-trans* receptors (*tttt*-1–3) to the corresponding *cis*-enriched mixtures in dichloromethane solution. We performed Isothermal Titration Calorimetry (ITC) experiments to accurately measure the binding constants of *all-trans* isomers of receptors 1–3 and their respective PSS mixtures with methyl trioctylammonium chloride (MTOA-Cl) in dichloromethane solution. Finally, we assessed the chloride transport activity of the receptors using large unilamellar vesicles (LUVs), carrier pre-insertion method and monitoring through HPTS and luciferin assays.

Results and discussion

Synthetic procedures

meso-Tetra-azobenzene-tetra-methyl C[4]P receptors 1–3 (Fig. 1) were synthesized using Baeyer–Mills reaction.²⁵ The procedure used was similar to the one reported previously for the synthesis of the unsubstituted tetra-azobenzene-tetra-ester analog.¹⁶ Unpurified labile nitrosoarene derivatives SD-SF were reacted with $\alpha,\alpha,\alpha,\alpha$ -tetra-phenylamino-tetra-methyl C[4]P S4 in acetic acid for constructing the diazene function of the *meso*-azobenzene substituents (see ESI†). The tetra-azobenzene-tetra-methyl calix[4]pyrroles C[4]P 1–3 were obtained as mixtures of *cis-trans* stereoisomers in 10 to 55% yield after column chromatography purification of the reaction crudes (1–3). In the case of receptor 2, the isolated product required further purification by precipitation from a DCM : MeOH 2 : 1 solvent mixture (see ESI† for details).

The fluoro-azobenzene S5 was prepared as reference compound by reacting 4-pentylbenzeneamine with methyl 4-fluoro-3-nitrosobenzoate.

In turn, the nitrosoarene derivatives SD-SF (ESI†) were obtained by Oxone® mediated oxidation of the parent phenylani-



lines in a DCM:H₂O (2:8) solvent mixture. The isolated nitrosoarene derivatives were used without further purification.

All compounds except the nitrosoarene derivatives were characterized by a complete set of high-resolution spectra (NMR and HRMS) (see ESI† for details).

Photo-isomerization studies

We studied the *trans*-to-*cis* photo-isomerization of the azobenzene units of the prepared C[4]Ps 1–3 in dichloromethane solution by means of UV-Vis and ¹H NMR spectroscopy. The spectroscopic signatures of the *trans*-to-*cis* isomerization processes were similar to those previously reported for the tetra-azobenzene-tetra-ester counterpart unsubstituted at its upper rim.¹⁶

The UV-Vis spectrum of a thermally equilibrated (2 days at rt in the dark) dichloromethane solution of C[4]P 3 (100 μM) showed an intense absorption band with a maximum at 335 nm (red line in Fig. 2). This band was attributed to the allowed $\pi \rightarrow \pi^*$ transition of the *meso*-azobenzene units in *trans* conformation.²⁶ Photo-irradiation of the solution with 365 nm light produced a strong decrease in the intensity of the absorption band at 335 nm. Simultaneously, a new band centered around 450 nm grew in intensity. This new band was assigned to the $n \rightarrow \pi^*$ transition of the *cis*-isomers of the *meso*-azobenzene substituents.²⁷ The observed changes were in complete agreement with the *trans*- to *cis*-isomerization process of the *meso*-azobenzene units of 3.²⁸

After 40 s of UV irradiation (orange line in Fig. 2) the photo-stationary state (PSS) was reached owing to the dilute conditions of the sample. The photo-isomerization process *tttt*-3 should result in a PSS containing a mixture of *cis*-enriched isomers (e.g. *cccc*-, *tttc*-, *ttcc*-, *tctc*- and *tccc*- isomers). The original UV-Vis spectrum was recovered after thermal equilibration of the photo-irradiated solution mixture at rt in the dark for 2 days.

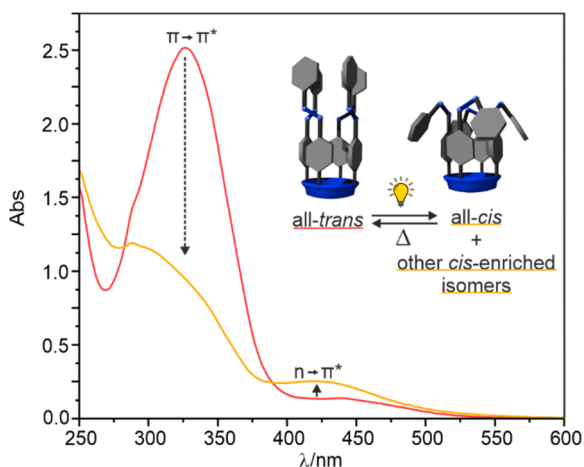


Fig. 2 UV-Vis spectra of a 100 μM DCM solution of 3 before and after light irradiation ($\lambda_{\text{exc}} = 365$ nm). The observed changes in the spectra are diagnostic of *trans*-to-*cis* isomerization of the azobenzene group. Red line – thermo-equilibrated sample; Orange line – PSS.

We also monitored the photo-isomerization process of 3 by ¹H NMR spectroscopy. The ¹H NMR spectrum of a 2 mM thermally equilibrated solution of 3 in CD₂Cl₂ showed a single set of sharp and well-resolved proton signals in agreement with a *C*_{4v} symmetry. Additionally, the ¹⁹F NMR spectrum displayed a single sharp singlet resonating at $\delta = -117.9$ ppm. Taken together, these observations indicated the exclusive detection of the all-*trans* isomer 3 in solution using ¹H and ¹⁹F NMR spectroscopy (Fig. 3, bottom spectra).

Next, the solution in the NMR tube was *ex situ* irradiated with UV-light ($\lambda_{\text{exc}} = 365$ nm) at regular intervals of time (10, 20, 30 and 40 s). The progress of the photo-induced isomerization reaction was monitored using ¹H and ¹⁹F NMR spectroscopy. We observed a decrease in intensity of the proton signals assigned to the all-*trans* isomer of 3. Concomitantly, we observed the appearance of new and complex sets of proton signals increasing at the expense of the former. In addition, the ¹⁹F NMR spectra showed a decrease in intensity of the singlet attributed to the fluorine atom for the all-*trans* 3 (~ -118 ppm) and the simultaneous increase of multiple singlets that were downfield shifted (~ -115 ppm) compared to the former (Fig. 3 bottom). Altogether, these observations suggest the formation of a mixture of *cis*-enriched isomers of 3 upon irradiation. After 40 s of UV-light irradiation, we did not observe additional changes in the ¹H and ¹⁹F NMR spectra, indicating that the PSS had been reached. At this point, the integral values of the fluorine signals corresponding to *meso*-

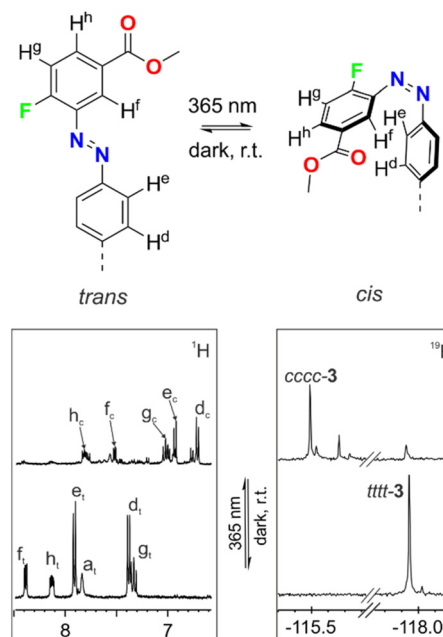


Fig. 3 (Top) *Trans*-to-*cis* isomerization process of *meso*-azo-benzene substituents of 3 and the corresponding proton assignment. (Bottom) Selected regions of the ¹H and ¹⁹F NMR spectra (400 MHz, 376 MHz, CD₂Cl₂, 298 K) of a solution of 3 (2 mM) thermally equilibrated (bottom) and after *ex situ* light irradiation with a LED at 365 nm for 40 s (top). "t" and "c" subscripts refer to the receptor in the *tttt*- and *cccc*-conformation, respectively.



substituents of **3** in *cis*-form and that of the singlet corresponding to the *trans* counterpart assigned a *trans*-to-*cis* isomerization ratio of 80% for the azobenzene units installed in the C[4]P. This value is in good agreement with that determined for the photo-isomerization of the azobenzene groups in the model compound **S5** (Fig. S26[†]). The obtained results suggested that each *meso*-azobenzene substituent in **3** experienced an independent photo-isomerization process.

Remarkably, one set of proton signals, in agreement with C_{4v} symmetry, showed a prevalent intensity in the ^1H and ^{19}F NMR spectra of the PSS of **3**. We assigned this set of signals to the all-*cis* isomer of **3** (Fig. 3, top). The most significant chemical shift changes experienced during light irradiation corresponded to the aromatic protons *ortho* to the azo group in both phenyl substituents, H^f and H^e . These signals experienced significant upfield shifts with $\Delta\delta$ values between *tttt*-**3** and *cccc*-**3** of -0.64 and -0.84 ppm, respectively.

As previously observed using UV-Vis spectroscopy, the thermal equilibration of the irradiated NMR tube containing the enriched mixture of *cis*-isomers of **3** at rt in the dark for 2 days reverted to the original ^1H NMR spectrum of all-*trans* **3**. In short, thermal equilibration reset the four photo-switches of **3** to their *trans*-form.

In conclusion, the results of light irradiation experiments monitored by UV-Vis and NMR spectroscopy evidenced that the *trans*-to-*cis* photo-isomerization process of the *meso*-azobenzene units of **3** was reversible and that the C[4]P was photo-stable under the described conditions. The photo-isomerization studies performed with C[4]P **1** and **2** produced analogous changes in their UV-Vis and NMR spectra (see ESI, Fig. S21 and S22[†]).

Binding studies of tetra-azobenzene C[4]P receptors with MTOA-Cl in dichloromethane solution: photo-control of chloride binding affinity

Next, we evaluated the binding properties of the all-*trans* and *cis*-enriched forms of the synthesized tetra-azo receptors **1**–**3** using methyl trioctylammonium chloride (MTOA-Cl) as chloride precursor and dichloromethane or its deuterated version CD_2Cl_2 as solvent.

First, we performed ^1H NMR titrations to probe the interaction of the salt with the C[4]P receptors. In all cases, the incremental addition of MTOA-Cl to a 2 mM thermally equilibrated solution of the receptor in CD_2Cl_2 provoked the appearance of a new set of proton signals for the receptor. We assigned the new set of signals to the protons of the bound receptor. The new set of signals grew at the expense of those of the free receptor (Fig. 4 and Fig. S27–S29[†]). We observed the emergence of a broad signal resonating at $\delta = 11.8$ ppm. We attributed this signal to the NH's protons of the bound receptor. The large downfield shift experienced by these protons compared to the free counterpart ($\Delta\delta \sim 3$ – 4 ppm) suggested their involvement in hydrogen bonding interactions. In the presence of 1 equiv. of MTOA-Cl, we exclusively observed the set of signals attributed to the bound receptor (Fig. 4c). Similarly, for the titration experiments with receptor **3**, the ^{19}F

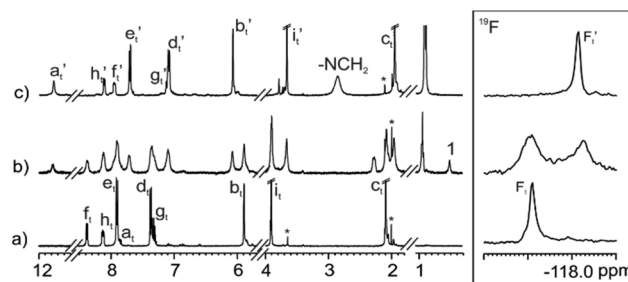


Fig. 4 Selected regions of the ^1H and ^{19}F NMR (CD_2Cl_2 , 400 MHz, 376 MHz, 298 K) of a thermally equilibrated solution of **3** (2 mM) with (a) 0; (b) 0.4 and (c) 1 equiv. of MTOA-Cl. "t" subscript refers to the receptor in the *tttt*-conformation. Primed letters correspond to the proton signals of bound species in the (MTOA-Cl)_t*tttt*-**3** complex. See Fig. 1 and 3 for proton assignments.

NMR spectrum after the addition of 0.4 equiv. of MTOA-Cl showed separate signals for the free and bound receptor. In the presence of equimolar amounts of receptor **3** and MTOA-Cl only one singlet resonating at -118.1 ppm (F_t) was observed. We attributed this observation to the quantitative binding of the ion-pair to the C[4]receptor. Analogous results were obtained with C[4]Ps **1** and **2**.

Taken together, the results described above indicated that the binding equilibria of C[4]P receptors **1**–**3** with MTOA-Cl featured slow chemical exchange dynamics on the chemical shift time scale. The all-*trans* C[4]P receptors formed 1 : 1 complexes with chloride for which we estimated binding constants larger than 10^4 M^{-1} .^{29,30}

Remarkably, after the addition of 0.4 equiv. of MTOA-Cl, the protons of the methyl alpha to the nitrogen atom of the MTOA⁺ cation (H^1) resonated around $\delta = 0.5$ ppm (Fig. 4b). The addition of increasing amounts of the MTOA-Cl provoked a gradual broadening and downfield shift of this signal. This observation was indicative of the binding of the MTOA⁺ cation by the C[4]P. The MTOA⁺ cation inserted its methyl group alpha to the nitrogen in the shallow and electron-rich cavity defined by the pyrrole rings in the cone conformation of the receptor. The binding site of the MTOA⁺ cation is opposed to that of the bound chloride resulting in a 1 : 1 : 1 ion-paired complex with receptor-separated binding geometry.^{31,32} In addition, the two components of the ion-pair complex featured interactions with the C[4]P receptors **1**–**3** of significantly different strength. The chloride established four convergent hydrogen bonds and additional chloride- π interactions. The MTOA⁺ cation is mainly bound to the receptor by cation- π interactions. The different strength of the established interactions between the anion/cation and the C[4]P receptors served to explain why the dynamics of the binding processes with chloride and MTOA⁺ are different, slow and fast on the chemical shift timescale, respectively.

We performed analogous titration experiments using light irradiated solutions of the C[4]P receptors that had reached their PSS. Similarly, to the results obtained for the all-*trans*-isomers, the addition of less than 1 equiv. of MTOA-Cl to the



cis-enriched mixture of the C[4]P receptors in CD₂Cl₂ solution produced the observation of separate signals for the free and bound receptor. After the addition of 1 equiv. of MTOA-Cl only the signals attributed to the *cis*-enriched isomeric bound receptors were observed. This result assigned an average binding constant larger than 10⁴ M⁻¹ for the 1 : 1 : 1 ion-paired complexes of the *cis*-enriched mixture of isomers. The ion-paired nature of the complexes of the *cis*-enriched isomers was substantiated by the observed chemical shift value for the protons of the methyl group alpha to the nitrogen atom of the MTOA⁺ cation resonating at $\delta \sim 0.6$ ppm (H¹) in the early stages of the titration (<0.3 equiv., Fig. S30†).

In order to determine more accurate binding constants for the all-*trans* C[4]P receptors and their corresponding *cis*-enriched mixtures at the PSS, we performed ITC experiments. The computer controlled sequential injection of a CH₂Cl₂ solution of MTOA-Cl to an 8 to 10-fold more diluted solution of the tetra-azobenzene-C[4]P receptors 1–3 in the same solvent placed in the calorimeter cell produced a gradual release of heat (Fig. S32–S34†). The normalized integrated heat values described a mono-sigmoidal binding isotherm with an inflexion point centered at a molar ratio MTOA-Cl/C[4]P equal to 1. We fit the experimental data to a theoretical 1 : 1 binding mode using the “one set of sites” model implemented in the Microcal analysis software.§

Table 1 summarizes the thermodynamic parameters of the binding processes of MTOA-Cl with the C[4]P receptors' series determined from the ITC experiments. We draw several conclusions from the tabulated data. Firstly, the all-*trans* isomers of all C[4]P receptors displayed binding constants of the order of 10⁵ M⁻¹ for the binding of MTOA-Cl in CH₂Cl₂ solution. The binding events were mainly driven by enthalpy with a favorable contribution of the entropic term. This latter result suggested that important solvation/desolvation effects were involved in the binding processes.

Secondly, for any given receptor, the binding constant decreased by approximately 4-fold when comparing the PSS

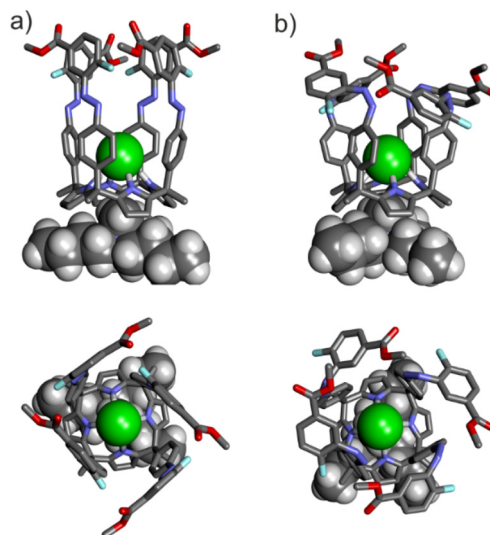


Fig. 5 Side and top views of the energy minimized structures (BP86-D3/def2-SVP) of the 1 : 1 : 1 complexes of (a) (MTOA-Cl)⁺-C[4]P-tttt-3 and (b) (MTOA-Cl)⁺-C[4]P-cccc-3. We placed 2 implicit molecules of dichloromethane in the cavity of the two ion-paired isomeric complexes. The two molecules of dichloromethane were removed from the picture for clarity.

mixture of *cis*-enriched isomers to the all-*trans* counterpart. The decrease in the binding constant was attributed to a reduction in the enthalpic term. However, the contribution of entropy was also favorable and slightly larger than for the binding of the all-*trans* isomers.¶

To gain some insight on the structures and energy differences of the 1 : 1 : 1 complexes formed between the MTOA-Cl and the all-*trans* and all-*cis* isomers of tetra-azobenzene C[4]P receptors we performed DFT calculations at the BP86^{33,34}-D3³⁵/def2-SVP level of theory using Turbomole v7.0. In particular, we computed the electronic energies and structures of the complexes of *tttt*-1, *cccc*-1, *tttt*-3 and *cccc*-3 (Fig. 5 and Fig. S35†). The computed energetic preference for the all-*trans* over all-*cis* ($\Delta E_{\text{tttt-cccc}}$) complexes agreed with their experimentally measured relative thermodynamic stabilities ($\Delta\Delta G = RT \ln K_{\text{tttt}}/K_{\text{cccc}}$) (see ESI†).

The computational results also revealed the existence of a significant difference in dipole moments for the two isomeric complexes (Table S1†). The dipole moment for the *tttt*-isomers was larger than for the *cccc*-counterparts ($\Delta(\text{dipole moments}_{\text{tttt-cccc}}) \sim 2$ D).

We also computed the electrostatic surface potential (ESP) of the free calix[4]pyrrole walls upon photo-isomerization (Fig. S36 and S37†). We used the *cis*- and *trans*-forms of a simple functionalized azobenzene as models to study the changes occurring in the electrostatic surface potentials (ESP) of the azobenzene walls of the C[4]P receptors upon photo-isomerization (see the ESI† for details). The ESP values at the

Table 1 Association constant values (K_a (M⁻¹)) and thermodynamic parameters (ΔH , $T\Delta S$ and ΔG (kcal mol⁻¹)) for the complexation of receptors 1–3 with MTOA-Cl in dichloromethane derived from ITC experiments

	$K_a/10^4$	ΔG	ΔH	$T\Delta S$	$K_{\text{tttt}}/K_{\text{PSS}}$
1- <i>tttt</i>	7.6 ± 0.5	−6.5 ± 0.04	−4.8 ± 0.09	1.7 ± 0.5	4.2 ± 1
1-PSS	1.9 ± 0.5	−5.7 ± 0.2	−3.2 ± 0.1	2.6 ± 0.8	
2- <i>tttt</i>	11.6 ± 0.9	−6.7 ± 0.1	−5.2 ± 0.2	1.5 ± 0.3	3.7 ± 0.4
2-PSS	3.1 ± 0.3	−6.1 ± 0.1	−3.0 ± 0.3	3.1 ± 0.3	
3- <i>tttt</i>	8.0 ± 1.4	−6.5 ± 0.1	−3.9 ± 0.1	2.6 ± 0.1	4.2 ± 0.8
3-PSS	1.9 ± 0.1	−5.7 ± 0.03	−2.3 ± 0.2	3.4 ± 0.1	

§ The ¹⁹F NMR spectrum recorded after the ITC experiment of the PSS-mixture of 3 with MTOA-Cl showed that *cis*-enriched-3 did not isomerize back significantly to the thermodynamically stable *trans*-isomer during the titration (Fig. S31†). We assumed a similar behaviour for the other receptors.

¶ Analogous experiments performed in acetone provided binding constants one order of magnitude lower than the ones determined in DCM. However, the $K_{\text{tttt}}/K_{\text{PSS}}$ ratios in acetone are similar to those reported in DCM.



center of the aromatic rings of the model azobenzenes did not show significant differences between the *trans*- and *cis*-forms (<1 kcal mol $^{-1}$) (Table S2†). In contrast, the ESP value at the center of the diazene bond, N=N, in the *cis*-isomers showed more negative values than the *trans*-counterparts (~ 20 kcal mol $^{-1}$) (Table S2†). Most likely, different electrostatic interactions between the chloride bound in the *cis*-enriched C[4]P receptors are responsible for the reduced thermodynamic stability of the resulting complexes.

To sum up, light irradiation caused the *trans*-to-*cis* isomerization of the azobenzene walls in C[4]Ps 1–3 to an 80% ratio. We also quantified the binding constants for MTOA-Cl in dichloromethane solution revealing a four-fold difference in binding between the all-*trans* and the *cis*-enriched mixture of isomers at the PSS. In short, the efficient photo-induced isomerization process was not coupled to a significant difference in binding affinity for chloride between isomeric receptors.

Photo-control of chloride transport studies across liposomal membranes using tetra-azobenzene C[4]P receptors as carriers

We were curious to investigate if the reduced 4-fold difference in chloride binding affinity between the photo-addressable states of the tetra-azobenzene extended C[4]Ps could be used to modulate the transport of chloride across a liposomal bilayer.

First, we evaluated the chloride transport properties of the C[4]P carriers 1–3 using standard 8-hydroxypyrene-1,3,6-trisulfonic acid (HPTS) assays (see the experimental section for details) (Fig. 6A). We prepared large unilamellar vesicles (LUVs) of 100 nm (mean diameter) from egg-yolk phosphatidylcholine (EYPC) lipid that were loaded with the fluorescent pH reporter.³⁶ We incorporated the carriers into the liposomal membranes using the pre-insertion method.¹⁰ The intra- and extra-vesicular media were buffered with NaCl (100 mM) and HEPES (10 mM) at pH 7. The pH gradient was generated by the addition of a pulse of NaOH and the dissipation of the intra-vesicular pH gradient (through H $^{+}$ /Cl $^{-}$ symport or Cl $^{-}$ /OH $^{-}$ antiport) was monitored using fluorescence measurements (λ_{exc} = 450 nm and λ_{em} = 510 nm).

Table 2 Chloride transport properties of carriers 1–3 (*tttt*-isomers and PSS' mixtures) pre-inserted in EYPC-LUVs derived from the HPTS assays

	v_{ini}^a (% s $^{-1}$)	n^b	EC $_{50}^c$ (nM)	F^d
1- <i>tttt</i>	1.3 \pm 0.1	0.9 \pm 0.1	5.6 \pm 0.5	4.5 \pm 0.9
1-PSS	0.5 \pm 0.1	1.1 \pm 0.3	25.7 \pm 4.9	
2- <i>tttt</i>	0.8 \pm 0.1	0.8 \pm 0.2	7.6 \pm 1.7	4.7 \pm 1.3
2-PSS	0.4 \pm 0.1	1.0 \pm 0.1	36.0 \pm 5.7	
3- <i>tttt</i>	1.1 \pm 0.1	1.4 \pm 0.5	5.0 \pm 1.1	3.4 \pm 0.9
3-PSS	0.6 \pm 0.1	0.8 \pm 0.1	17.0 \pm 2.6	

^a Initial rate determined at 0.15% carrier/lipid molar ratio. ^b Hill coefficient. ^c Effective concentration of the receptor needed for 50% transport activity. ^d Factor of enhancement between the transport of irradiated and non-irradiated LUVs calculated as $F = \text{EC}_{50}(\text{PSS})/\text{EC}_{50}(\text{tttt})$.

tidylcholine (EYPC) lipid that were loaded with the fluorescent pH reporter.³⁶ We incorporated the carriers into the liposomal membranes using the pre-insertion method.¹⁰ The intra- and extra-vesicular media were buffered with NaCl (100 mM) and HEPES (10 mM) at pH 7. The pH gradient was generated by the addition of a pulse of NaOH and the dissipation of the intra-vesicular pH gradient (through H $^{+}$ /Cl $^{-}$ symport or Cl $^{-}$ /OH $^{-}$ antiport) was monitored using fluorescence measurements (λ_{exc} = 450 nm and λ_{em} = 510 nm).

The evaluation of the transport efficiency of the all-*trans* carriers was performed using thermally equilibrated suspensions of liposomes (24 h rt in the dark) with the carriers already embedded in their membranes. For the assessment of *cis*-enriched mixtures at the PSS, the vesicles' suspensions with pre-inserted receptor carriers were "*in situ*" irradiated with 365 nm light for 60 s just before the addition of the base pulse.||

In order to probe the photo-stability of the prepared liposomes we undertook control transport experiments (Fig. S38†). The obtained results showed that the passive diffusion of Cl $^{-}$ anions through the membranes of liposomes lacking inserted carriers in their membranes was almost identical for the irradiated (365 nm for 60 s) and non-irradiated sample. This finding was used to sustain the photo-stability of the pristine liposomes under the described experimental conditions of irradiation.

Fig. 6B shows the fluorescence time-course curves of the HPTS chloride transport experiments performed using carrier 3 (*tttt*-3 and PSS'-3) at 0.15% carrier/lipid molar ratio. To better assess and compare the transport activities of the carriers we calculated the initial transport rate (v_{ini}) of chloride efflux (pH dissipation) by linearly fitting the data of fluorescence vs. time at the initial transport stage (0–25 s) (Fig. S45†). The results of the transport studies are summarized in Table 2.

On the one hand, we determined double initial transport rates for chloride comparing liposomes having the all-*trans*-

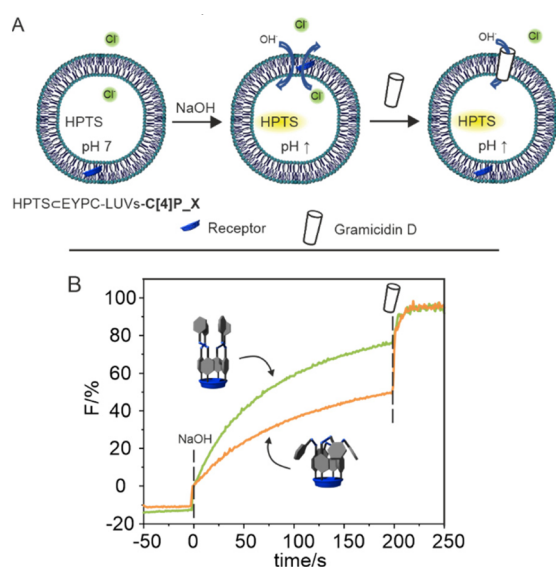


Fig. 6 (A) Schematic representation of the HPTS assay used to evaluate the chloride transport efficiency of the tetra-azobenzene C[4]P carriers 1–3. (B) Fluorescence time-course curves of chloride transport experiments using LUVs with pre-inserted carrier 3 at 0.15% carrier/EYPC molar ratio. Green line – all-*trans*; orange line – *cis*-enriched mixture after 60 s UV-light irradiation.

|| We refer to the *cis*-enriched mixture of tetra-azobenzene C[4]Ps inserted in the liposomal after 60 s of light irradiation as PSS'. We were not able to quantify the composition of the mixture present in the membranes but we assume that it is similar to the one determined in solution.



carriers inserted to those previously light irradiated and containing the *cis*-enriched mixture of carriers at PSS'. At the same carrier/lipid molar ratio, the initial transport rates of the all-*trans*-carriers were similar to that previously reported by us for a "four wall" aryl extended calix[4]pyrrole as carrier (1.76% s⁻¹).¹⁰ On the other hand, the relative fluorescence values (%*F*) achieved at the end of the transport experiments, that is just before the addition of Gramicidin D (*t* = 200 s), were ~1.5 larger in the case of thermally equilibrated LUVs having the all-*trans*-carriers inserted in the membrane. Overall, the obtained results highlighted that the chloride transport efficiency of the all-*trans*-isomers of all receptors was larger than that of their respective *cis*-enriched-mixtures at the PSS'.

We performed dose-response chloride transport studies with the different carriers in their all-*trans*- and PSS'-states (Fig. S39–S44†). The analysis of the experimental data using Hill's equation (see ESI†) assigned a Hill coefficient (*n*-value in Table 2) close to 1 for all cases. This suggested the putative formation of carrier:chloride complex of 1:1 stoichiometry in the membrane as previously observed in solution. Moreover, and in agreement with their larger transport activity, the determined half-maximal effective concentrations (EC₅₀) for the all-*trans*-isomers of the carriers were smaller than those of the PSS' counterpart.

We calculated an enhancement factor between irradiated and non-irradiated LUVs (EC_{50(PSS)'}/EC_{50(*ttt*)}) of approximately 4–5 folds for the all-*trans*-isomers of the three carriers. This value showed a good correlation with the photo-modulated ratio of binding constants (*K*_{*ttt*}/*K*_{PSS}) determined in solution for the all-*trans*-isomers and their corresponding *cis*-enriched mixtures at the PSSs (*vide supra*).

Finally, in order to support that the transport ability of the tetra-azo-benzene C[4]P carriers was intrinsic for chloride, we performed additional transport studies using the lucigenin assay.^{33,37} In this assay, the diffusion of chloride anions through the liposomal membrane and into the intra-vesicular medium results in the quenching of the fluorescence of the chloride-sensitive lucigenin dye.³⁸ We prepared POPC:cholesterol 7:3 LUVs loaded with lucigenin dye and containing pre-inserted carrier 3 at two different carrier/lipid molar ratio (0.1 and 0.05%). The chloride transport was initiated by the addition of concentrated NaCl (25 mM) to the extra-vesicular medium and the fluorescence emission at 535 nm (*λ*_{exc} = 450 nm) was monitored.

The results obtained in the lucigenin assays were in complete agreement with those derived from the HPTS assays. On the one hand, a higher carrier loading (control, 0.05% and 0.1%) increased the rate of the mediated chloride transport. On the other hand, the *ttt*-3 isomer of the carrier displayed a larger transport efficiency (in this case directly attributed to the chloride influx) than the corresponding mixture of *cis*-enriched-3 carriers at the PSS' (Fig. S46†).

We compared the results obtained from the lucigenin assay for 0.1% loading of *ttt*-3 with that reported previously by us

using the same method and loading for a tetra-nitro aryl extended C[4]P carrier.¹⁰ The values of the fluorescence change %Δ*F* after 500 s for the two carriers were similar indicating a similar chloride transport efficiency. It is worth mentioning here, that these and others C[4]Ps carriers featured low transport activity for chloride in the lucigenin assay in comparison to several other families of synthetic carriers reported in the literature.³⁹

Conclusions

We described the synthesis and characterization of three α,α,α,α-C[4]P receptors 1–3 bearing four *meso*-azobenzene units differently substituted at the terminal phenyl ring (upper rim). We studied their photo-isomerization properties in dichloromethane solution using UV-Vis and NMR spectroscopy. The azobenzene moiety in the C[4]P scaffolds reached a *trans*-to-*cis* isomerization ratio of 80% at the PSS indicating that they experienced an independent photo-isomerization process. We assessed the binding properties of the all-*trans*-isomers and their corresponding *cis*-enriched mixtures at the PSS toward MTOA-Cl, as chloride source, in dichloromethane solution. In all cases, the receptors formed 1:1:1 ion-paired complexes displaying a receptor-separated binding geometry. That is, the chloride anion is included in the aromatic cavity of the receptors by establishing four convergent hydrogen bonding interactions with the pyrrole NH protons. The MTOA⁺ cation is bound in the shallow electron-rich cavity, opposed to the bound anion, defined by the pyrrole rings in the cone conformation of the C[4]P.

We determined a 4-fold photo-modulation in chloride binding affinity for the photo-isomers of the 1–3 C[4]P receptors. We attributed this difference to dissimilar electrostatic interactions in the complexes. The ESP values at the center of the diazene N=N bond computed for the *cis*- and *trans*-forms of model compounds were significantly different.

Finally, using HPTS and lucigenin assays, we showed that the measured differences in binding affinity of the all-*trans*- and the PSS-states of the receptors were transferred into dissimilar chloride transport activities. All-*trans*-isomeric carriers displayed a larger chloride transport efficiency than their corresponding mixture of *cis*-enriched isomers at the PSS'.

The described photo-active C[4]P carriers did not outperform the chloride transport efficiency of other synthetic carriers described in literature. Nevertheless, we expect that the reported results will be useful for the development of more efficient photo-controlled chloride synthetic transporters. In addition, the reported data could aid in discovering correlations between photo-modulation of chloride binding and photo-control in chloride transport activity using synthetic carriers.

Author contributions

Conceptualization, P. B.; methodology, P. F.; Computational studies P. B., G. A.; formal analysis, P. B., G. A.; writing – orig-

** Check the Experimental section (ESI†) for details.



inal draft, G. A. and P. F.; writing – review and editing, P. B. and G. A.; supervision, P. B. All authors have read and agreed to the published version of the manuscript.

Conflicts of interest

There are no conflicts to declare.

Acknowledgements

The authors thank the European Union (NOAH project H2020-MSCA-ITN project Ref. 765297), Ministerio de Ciencia e Innovación/Agencia Estatal de Investigación (MCIN/AEI/10.13039/501100011033) (PID2020-114020GB-I00 and CEX2019-000925-S), the CERCA Programme/Generalitat de Catalunya, AGAUR (2021SGR00851) and ICIQ Foundation.

References

- 1 H. Li, H. Valkenier, A. G. Thorne, C. M. Dias, J. A. Cooper, M. Kieffer, N. Busschaert, P. A. Gale, D. N. Sheppard and A. P. Davis, Anion carriers as potential treatments for cystic fibrosis: transport in cystic fibrosis cells, and additivity to channel-targeting drugs, *Chem. Sci.*, 2019, **10**, 9663–9672.
- 2 J. Yang, G. Yu, J. L. Sessler, I. Shin, P. A. Gale and F. Huang, Artificial transmembrane ion transporters as potential therapeutics, *Chem*, 2021, **7**, 3256–3291.
- 3 J. T. Davis, P. A. Gale and R. Quesada, Advances in anion transport and supramolecular medicinal chemistry, *Chem. Soc. Rev.*, 2020, **49**, 6056–6086.
- 4 X. Wu, A. M. Gilchrist and P. A. Gale, Prospects and Challenges in Anion Recognition and Transport, *Chem*, 2020, **6**, 1296–1309.
- 5 J. de Jong, J. E. Bos and S. J. Wezenberg, Stimulus-Controlled Anion Binding and Transport by Synthetic Receptors, *Chem. Rev.*, 2023, **123**, 8530–8574.
- 6 M. J. Langton, Engineering of stimuli-responsive lipid-bilayer membranes using supramolecular systems, *Nat. Rev. Chem.*, 2021, **5**, 46–61.
- 7 S. Lee and A. H. Flood, Photoresponsive receptors for binding and releasing anions, *J. Phys. Org. Chem.*, 2013, **26**, 79–86.
- 8 D.-H. Qu, Q.-C. Wang, Q.-W. Zhang, X. Ma and H. Tian, Photoresponsive Host–Guest Functional Systems, *Chem. Rev.*, 2015, **115**, 7543–7588.
- 9 D. S. Kim and J. L. Sessler, Calix[4]pyrroles: versatile molecular containers with ion transport, recognition, and molecular switching functions, *Chem. Soc. Rev.*, 2015, **44**, 532–546.
- 10 L. Martínez-Crespo, J. L. Sun-Wang, P. Ferreira, C. F. M. Mirabella, G. Aragay and P. Ballester, Influence of the Insertion Method of Aryl-Extended Calix[4]pyrroles into Liposomal Membranes on Their Properties as Anion Carriers, *Chem. – Eur. J.*, 2019, **25**, 4775–4781.
- 11 L. Martínez-Crespo, J. L. Sun-Wang, A. F. Sierra, G. Aragay, E. Errasti-Murugarren, P. Bartoccioni, M. Palacín and P. Ballester, Facilitated Diffusion of Proline across Membranes of Liposomes and Living Cells by a Calix[4]pyrrole Cavitand, *Chem*, 2020, **6**, 3054–3070.
- 12 G. Cafeo, F. H. Kohnke, G. Mezzatesta, A. Profumo, C. Rosano, A. Villari and A. J. P. White, Host–Guest Chemistry of a Bis-Calix[4]pyrrole Derivative Containing a trans/cis-Switchable Azobenzene Unit with Several Aliphatic Bis-Carboxylates, *Chem. – Eur. J.*, 2015, **21**, 5323–5327.
- 13 L. Osorio-Planes, M. Espelt, M. A. Pericàs and P. Ballester, Reversible photocontrolled disintegration of a dimeric tetraurea-calix[4]pyrrole capsule with all-trans appended azobenzene units, *Chem. Sci.*, 2014, **5**, 4260–4264.
- 14 A. Díaz-Moscoso, F. A. Arroyave and P. Ballester, Moving systems of polar dimeric capsules out of thermal equilibrium by light irradiation, *Chem. Commun.*, 2016, **52**, 3046–3049.
- 15 P. Ferreira, G. Monceli, G. Aragay and P. Ballester, Hydrogen-Bonded Dimeric Capsules with Appended Spiropyran Units: Towards Controlled Cargo Release, *Chem. – Eur. J.*, 2021, **27**, 12675–12685.
- 16 L. Escobar, F. A. Arroyave and P. Ballester, Synthesis and Binding Studies of a Tetra- α Aryl-Extended Photoresponsive Calix[4]pyrrole Receptor Bearing meso-Alkyl Substituents, *Eur. J. Org. Chem.*, 2018, 1097–1106.
- 17 V. Jain and D. H. Mandalia, Azocalix[4]pyrroles: One-pot microwave and one drop water assisted synthesis, spectroscopic characterization and preliminary investigation of its complexation with copper(II), *J. Inclusion Phenom. Macrocyclic Chem.*, 2009, **63**, 27–35.
- 18 V. K. Jain, H. C. Mandalia and N. Bhojak, Azocalix[4]pyrrole dyes: Application in dyeing of fibers and their antimicrobial activity, *Fibers Polym.*, 2010, **11**, 363–371.
- 19 D. Villarón, M. A. Siegler and S. J. Wezenberg, A photoswitchable strapped calix[4]pyrrole receptor: highly effective chloride binding and release, *Chem. Sci.*, 2021, **12**, 3188–3193.
- 20 D. Villarón, G. E. A. Brugman, M. A. Siegler and S. J. Wezenberg, Photoswitching of halide-binding affinity and selectivity in dithienylethene-strapped calix[4]pyrrole, *Chem. Commun.*, 2023, **59**, 8688–8691.
- 21 Y. R. Choi, G. C. Kim, H.-G. Jeon, J. Park, W. Namkung and K.-S. Jeong, Azobenzene-based chloride transporters with light-controllable activities, *Chem. Commun.*, 2014, **50**, 15305–15308.
- 22 K. Dąbrowa, P. Niedbała and J. Jurczak, Anion-tunable control of thermal Z→E isomerisation in basic azobenzene receptors, *Chem. Commun.*, 2014, **50**, 15748–15751.
- 23 M. Ahmad, S. Metya, A. Das and P. Talukdar, A Sandwich Azobenzene–Diamide Dimer for Photoregulated Chloride Transport, *Chem. – Eur. J.*, 2020, **26**, 8703–8708.
- 24 N. Busschaert, I. L. Kirby, S. Young, S. J. Coles, P. N. Horton, M. E. Light and P. A. Gale, Squaramides as



- Potent Transmembrane Anion Transporters, *Angew. Chem., Int. Ed.*, 2012, **51**, 4426–4430.
- 25 E. Merino, Synthesis of azobenzenes: the coloured pieces of molecular materials, *Chem. Soc. Rev.*, 2011, **40**, 3835–3853.
 - 26 R. J. Sension, S. T. Repinec, A. Z. Szarka and R. M. Hochstrasser, Femtosecond laser studies of the cis-stilbene photoisomerization reactions, *J. Chem. Phys.*, 1993, **98**, 6291–6315.
 - 27 T. Nägele, R. Hoche, W. Zinth and J. Wachtveitl, Femtosecond photoisomerization of cis-azobenzene, *Chem. Phys. Lett.*, 1997, **272**, 489–495.
 - 28 C. L. Forber, E. C. Kelusky, N. J. Bunce and M. C. Zerner, Electronic spectra of cis- and trans-azobenzenes: consequences of ortho substitution, *J. Am. Chem. Soc.*, 1985, **107**, 5884–5890.
 - 29 M. Ciardi, F. Tancini, G. Gil-Ramírez, E. C. Escudero Adán, C. Massera, E. Dalcanale and P. Ballester, Switching from Separated to Contact Ion-Pair Binding Modes with Diastereomeric Calix[4]pyrrole Bis-phosphonate Receptors, *J. Am. Chem. Soc.*, 2012, **134**, 13121–13132.
 - 30 S. K. Kim and J. L. Sessler, Calix[4]pyrrole-Based Ion Pair Receptors, *Acc. Chem. Res.*, 2014, **47**, 2525–2536.
 - 31 R. Molina-Muriel, G. Aragay, E. C. Escudero-Adán and P. Ballester, Switching from Negative-Cooperativity to No-Cooperativity in the Binding of Ion-Pair Dimers by a Bis(calix[4]pyrrole) Macrocycle, *J. Org. Chem.*, 2018, **83**, 13507–13514.
 - 32 V. Valderrey, E. C. Escudero-Adán and P. Ballester, Highly Cooperative Binding of Ion-Pair Dimers and Ion Quartets by a Bis(calix[4]pyrrole) Macrotricyclic Receptor, *Angew. Chem., Int. Ed.*, 2013, **52**, 6898–6902.
 - 33 A. D. Becke, Density-functional exchange-energy approximation with correct asymptotic behavior, *Phys. Rev. A*, 1988, **38**, 3098–3100.
 - 34 J. P. Perdew, Density-functional approximation for the correlation energy of the inhomogeneous electron gas, *Phys. Rev. B: Condens. Matter Mater. Phys.*, 1986, **33**, 8822–8824.
 - 35 S. Grimme, J. Antony, S. Ehrlich and H. Krieg, A consistent and accurate ab initio parametrization of density functional dispersion correction (DFT-D) for the 94 elements H–Pu, *J. Chem. Phys.*, 2010, **132**, 154104.
 - 36 S. Matile and N. Sakai, The characterization of synthetic ion channels and pores, *Anal. Methods Supramol. Chem.*, 2006, 391–418.
 - 37 C. M. Dias, H. Valkenier and A. P. Davis, Anthracene Bisureas as Powerful and Accessible Anion Carriers, *Chem. – Eur. J.*, 2018, **24**, 6262–6268.
 - 38 B. A. McNally, A. V. Koulov, B. D. Smith, J.-B. Joos and A. P. Davis, A fluorescent assay for chloride transport; identification of a synthetic anionophore with improved activity, *Chem. Commun.*, 2005, 1087–1089, DOI: [10.1039/B414589E](https://doi.org/10.1039/B414589E).
 - 39 P. A. Gale, J. T. Davis and R. Quesada, Anion transport and supramolecular medicinal chemistry, *Chem. Soc. Rev.*, 2017, **46**, 2497–2519.

